

THE INFLUENCE OF A BLUFF BODY IN A TURBULENT FLOW ON THE MIXING OF FLUIDS

Toos VAN GOOL^{1*}, Oscar MEIJER^{2†}

¹University of Technology, Department of Mechanical Engineering, Eindhoven, NETHERLANDS

²University of Technology, Department of Mechanical Engineering, Eindhoven, NETHERLANDS

* E-mail: c.e.a.g.v.gool@student.tue.nl

† E-mail: o.c.meijer@student.tue.nl

ABSTRACT

This file is an example L^AT_EX file for submission to CFD2018. A limit of 15 pages applies (submitted file size < 10MB).

Keywords: CFD, Turbulence, Bluff body .

The first part of this article is composed of the theory and the numerical solver used to attain the solution. Then CFD model is treated, after which the Geometry and boundary conditions applied to the problem are discussed. Subsequently the mesh convergence and executed simulations are explained. Finally, the results of the simulations are displayed with a discussion and conclusion.

A complete list of symbols used, with dimensions, is required.

NOMENCLATURE

Greek Symbols

ρ Mass density, $[kg/m^3]$
 μ Dynamic viscosity, $[kg/ms]$

Latin Symbols

a PressureCharacteristic length, $[m]$.
 N Total amount, $[-]$.
 p Pressure, $[Pa]$.
 \mathbf{u} VolumeVelocity, $[m/s]$.

Sub/superscripts

G Gas.
 i Index i .
 j Index j .

INTRODUCTION

Within industrial applications, mixing of fluids is a well known phenomenon. Mixing fluids can be initiated by a propeller, driven by a motor, or by obstacles in a flow. A simple example is the mixing of two paint colors. starting with half a tank of blue paint and the other half yellow paint, will result in a completely green paint.

This study focusses on the quality of mixing. Mainly the influence of the bluff-body size and its influence on the mixing quality. The mixing quality can be measured at the outlet of the geometry by looking at the value of the mixture fraction. Computational Fluid Dynamics (CFD) is used to solve the system of equations. For this particular problem, the mass, momentum and transport equations are solved. The simulations are performed for fully developed turbulent and incompressible flows. The turbulence is modelled by means of a $\kappa - \epsilon$ model.

SOME PIECE ABOUT EXPECTATIONS??

PHYSICS

This chapter covers the theory behind the CFD model. Once the theory is explained, the discretization of the governing equations is treated. Additional to that the used solver is explained.

Turbulent flow

A flow in a channel can be characterized by the Reynolds number, a dimensionless number which represents the ratio of viscous and inertial forces in the flow. The Reynolds number can be calculated upon use of Equation 1 (Versteeg and Malalasekera, 2007). Here ρ is the fluid density in $[kg \cdot m^{-3}]$, u is the velocity in $[m \cdot s^{-1}]$, D is the characteristic length in $[m]$ and μ is the fluids dynamic viscosity in $[kg \cdot m^{-1} \cdot s^{-1}]$

$$Re = \frac{\rho u D}{\mu} \quad (1)$$

The flow is considered turbulent if the Reynolds number exceeds a value of 2300. A turbulent flow is contemplated as chaotic, containing flow instabilities such as eddies. These eddies cause local fluctuations in the velocity field. Therefore, the normal steady convection and diffusion equations can not be used to solve turbulent flows. To solve the turbulent flow equations one needs to introduce general equation for unsteady convection and diffusion (Versteeg and Malalasekera, 2007).

Unsteady convection-diffusion

$$\frac{\partial \rho \phi}{\partial t} + \text{div}(\rho \phi \mathbf{u}) = \text{div}(\Gamma \text{grad} \phi) + S_\phi \quad (2)$$

Equation 2 consists of four parts. The first part is the time dependent term, the second part represents the convection, the third part the diffusion and the last part of the equation is the sink and or source term. ϕ is the transport term, Γ is the diffusion or conduction coefficient. The transport term changes according to the equation to be solved.

The conservation of mass, momentum and fraction play a major role in a CFD code. All conservation equations are derived for the case of an incompressible flow. The conservation of mass can be extracted from Equation 2, and results in (Deen, 2017):

Mass balance

$$\frac{\partial \rho}{\partial t} + \text{div}(\rho \mathbf{u}) = 0 \quad (3)$$

For a two dimensional problem, the conservation of momentum needs to be solved in two directions, x and y . The general form for the momentum conservation is treated as:

Momentum balance

$$\begin{aligned} \frac{D(\rho u)}{Dt} &= -\frac{\partial P}{\partial x} + \text{div}(\mu \text{grad} u) + S_{Mx} \\ \frac{D(\rho u)}{Dt} &= -\frac{\partial P}{\partial x} + \text{div}(\mu \text{grad} u) + S_{Mx} \end{aligned} \quad (4)$$

The last important equation is the transport of fractions, and can be computed upon use of Equation 5.

Fraction transport

$$\rho C_p \frac{Df}{Dt} = \text{div}(k \text{grad} f) + S_i \quad (5)$$

DEZE MOET NOG IETS ANDERS!!!! The fraction transport is introduced specifically for this study in order to keep

track of the mixing of the flow.

Since this study regards a turbulent flow, the mass and momentum equations have to be solved in a different manner. This is done by taking the Reynolds average approach. In the Reynolds average approach the mean velocity is determined and the turbulence is described by a fluctuation around the mean velocity. Therefore, components in the convection-diffusion and conservation equations are decomposed in a mean and a fluctuation variable. The decomposed variables are given in Equation 6.

Decomposed variables

$$u = U + u'; \quad v = V + v'; \quad w = W + w'; \quad p = P + p' \quad (6)$$

In here, U , V and W are mean the velocities in x , y and z direction respectively. P is the average pressure. the apostrophe terms are the fluctuating components. The average term is given by Equation 7.

Average velocity

$$U = \frac{1}{\Delta t} \int_0^{\Delta t} u(t) dt \quad (7)$$

The other average terms are calculated in the same manner. After computing the decomposed variables, they are substituted into the system of equations. The time averaged part in Equation 7 transforms the regular Navier-Stokes equations into time averaged Navier-Stokes equations, also called Reynolds averaged Navier-Stokes equations (RANS). By using RANS, a new definition is introduced called Reynolds stresses. The Reynolds stresses are present in all directions, and are calculated by Equation 8 (Deen, 2017).

Reynolds stresses

$$\tau_{ij} = -\rho \overline{u'_i u'_j} \quad (8)$$

The $\kappa - \epsilon$ model is used to close the system of equations. The $\kappa - \epsilon$ is chosen above the Prandtl mixing length model and the Reynolds stress model and algebraic stress model due to its simple implementation and widely proven validation (Versteeg and Malalasekera, 2007).

$\kappa - \epsilon$ turbulence model

The standard $\kappa - \epsilon$ model introduces two extra transport equations to be solved. one for the turbulent kinetic energy, κ , and one for the viscous dissipation of turbulent kinetic energy, ϵ . κ and ϵ are used to introduce a velocity scale, θ and large-scale turbulence length scale ℓ . The velocity scale is calculated upon use of Equation 9, and the turbulence length-scale is calculated with use of Equation 10.

Velocity- and turbulence length-scale

$$\theta = \kappa^{1/2} \quad (9)$$

$$\ell = \frac{\kappa^{3/2}}{\epsilon} \quad (10)$$

Equation 10 shows that one is able to use the small eddy variable ϵ to describe the large eddy scale, ℓ . This is only permitted if, and only if, the rate at which large eddies extract energy from the mean flow matches the rate of transfer of energy across the energy spectrum to small, dissipating, eddies if the flow does not change rapidly. (Versteeg and Malalasekera, 2007).

The turbulent viscosity, the eddy viscosity is introduced by Equation 11, where C_μ is a dimensionless constant.

Turbulent viscosity

$$\mu_t = C_p \rho \theta \ell = C_p \rho \frac{\kappa^2}{\varepsilon} \quad (11)$$

One is now able to describe the equations for both κ and ε , shown in Equation 12 and 13 respectively.

κ - and ε -transport equation

$$\frac{\partial \rho \kappa}{\partial t} + \text{div}(\rho \kappa \mathbf{U}) = \text{div} \left[\frac{\mu_t}{\sigma_\kappa} \text{grad } \kappa \right] + 2\mu_t S_{ij} \cdot S_{ij} - \rho \varepsilon \quad (12)$$

$$\frac{\partial \rho \varepsilon}{\partial t} + \text{div}(\rho \varepsilon \mathbf{U}) = \text{div} \left[\frac{\mu_t}{\sigma_\varepsilon} \text{grad } \varepsilon \right] + C_{1\varepsilon} \frac{\varepsilon}{\kappa} 2\mu_t S_{ij} \cdot S_{ij} - \rho C_{2\varepsilon} \frac{\varepsilon^2}{\kappa} \quad (13)$$

In both equations, the first term represents the rate of change in κ and ε respectively. Within the first term \mathbf{U} is the average velocity magnitude. The second and third term represent the transport driven by convection and diffusion for κ and ε . The fourth and fifth term are the rate of production and rate of destruction of κ and ε .

The equations use five dimensionless constants, the standard $\kappa - \varepsilon$ model uses values that have been determined through comprehensive data fitting for a wide range of turbulent flows (Versteeg and Malalasekera, 2007):

Dimensionless constants:

$$C_\mu = 0.09 \quad \sigma_\kappa = 1.00 \quad \sigma_\varepsilon = 1.30 \quad C_{1\varepsilon} = 1.44 \quad C_{2\varepsilon} = 1.92$$

discretization of governing equations

To solve the turbulence model, all of the partial differential equations (PDE's) need to be solved. Solving a PDE takes a few steps. First of all let us consider a two dimensional grid consisting of several grid cells. To find the value for ϕ from Equation 2 at a centre point P of the grid cell, one needs the values of the neighbouring cells. In CFD these values are called north(N), west(W), south(S) and east(E). Thereafter, Equation 2 is integrated over the control volume, yielding the results shown in Equation 14. DEZE FUNCTIE NOG

EENS NAKIJKEN WANT DIE IS MOEILIK

Integrated diffusion convection equation

$$\begin{aligned} & \frac{(\rho_p^0) \phi}{\Delta t} \Delta V + [(\rho u A \phi)_e - (\rho u A \phi)_w] + [(\rho u A \phi)_n - \\ & (\rho u A \phi)_s] = \left[\left(\Gamma A \frac{\partial \phi}{\partial x} \right)_e - \left(\Gamma A \frac{\partial \phi}{\partial x} \right)_w \right] + \\ & \left[\left(\Gamma A \frac{\partial \phi}{\partial x} \right)_n - \left(\Gamma A \frac{\partial \phi}{\partial x} \right)_s \right] + S_u + S_p \phi_p^0 \end{aligned} \quad (14)$$

Now let us introduce variables F and D to represent the convective mass flux per unit area and the diffusive conductance at the cell faces (Versteeg and Malalasekera, 2007).

$$F = \rho u \quad (15)$$

$$D = \frac{\Gamma}{\partial x} \quad (16)$$

Substitution variables F and D into Equation 14 forms Equation 17 after some rearranging (Versteeg and Malalasekera,

2007).

OOK DEZE FORMULE NOG CHECKEN!!!

$$\frac{\rho_p^0 \Delta V}{\Delta t} \phi_P = a_W \phi_W + a_E \phi_E + a_S \phi_S + a_N \phi_N + \Delta F \quad (17)$$

The coefficients of a are dependent on the differencing scheme. The discretization scheme has some properties. First property is the conservativeness which means the flux ϕ leaving a control volume has to be equal to the flux ϕ entering the control volume through the same face. By using a hybrid differencing scheme, the conservativeness is automatically satisfied. The second property is the boundedness. The boundedness describes the value of ϕ in case there is no source term. In that case, the nodal value of ϕ must be equal to the value of ϕ at the boundary. Besides the restricted value of ϕ , the coefficients a of the discretized equation must have equal signs. The last important property is the transportiveness. This requires that the transportiveness changes according to the magnitude of the Péclet number ($Pe = F/D$). Hence, if Pe is zero, ϕ equally diffuses in all directions. The hybrid differencing scheme satisfies the three properties. However, this comes at the price of only first order accuracy (Versteeg and Malalasekera, 2007). The obtained values for F and D determine the values of the a coefficients. They can be determined as shown in Table 1.

Table 1: a coefficients.

| | Two-Dimensional Flow |
|------------|---|
| a_W | $\max \left[F_w, \left(D_w + \frac{F_w}{2}, 0 \right) \right]$ |
| a_E | $\max \left[-F_e, \left(D_e + \frac{F_e}{2}, 0 \right) \right]$ |
| a_N | $\max \left[-F_n, \left(D_n + \frac{F_n}{2}, 0 \right) \right]$ |
| a_S | $\max \left[F_s, \left(D_s + \frac{F_s}{2}, 0 \right) \right]$ |
| ΔF | $F_e - F_w + F_n - F_s$ |

The discretized equation can now be solved using the transient SIMPLE algorithm. SIMPLE stands for Semi-Implicit Method for Pressure-Linked Equations. In essential the algorithm is a guess and correct procedure for pressure calculations in a staggered grid which is used (Versteeg and Malalasekera, 2007). The transient SIMPLE algorithm is used due to the unsteady convection-diffusion equations used to describe the problem. The difference with the regular SIMPLE algorithm is the time t , discretized in time steps, Δt for which the equations are solved. The transient SIMPLE algorithm works in the following manner. First the variables u , v , p and ϕ are initialized and a time step Δt is defined. The time iteration starts at t_0 and continues until $t > t_{max}$. VERDERE UITLEG NODIG, EVEN GOED BEKIJKEN HOE DIE SOLVER WERKT

CFD PROBLEM

This chapter will describe the entire CFD model used during simulations. First of all the geometry will be introduces, after which the applied boundary conditions are explained.

Geometry and Cases

Figure 1 shows the geometry used during the research. The rectangular domain with dimensions length, L and width D , contains a bluff-body with height and width h and b respectively.

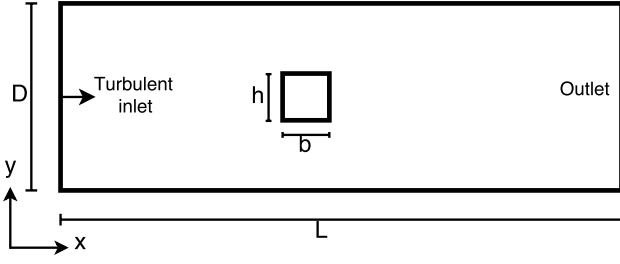


Figure 1: Schematic diagram of geometry.

For this research numerous cases are investigated. Since the main purpose is to find the influence of a bluff body on the mixing in a turbulent flow. The geometry of the bluff-body is varied from. The size of the bluff body is defined as h/D . The size is varied in three steps, linearly scaling from $h/D = XX$ to $h/D = XX2$. These results are compared to a flow without a bluff-body.

Besides varying the bluff-body size, the entrance turbulence intensity T_i and the inlet velocity U_{in} are varied.

Throughout the simulations the viscosity, turbulence entrance intensity and length scale and the density are not altered.

Boundary conditions

Boundary conditions are prescribed to this CFD problem. Since this study focusses on turbulent flows only, the applied boundary conditions are solely turbulent as well. First of all A fully developed turbulent profile enters the geometry at the left side. This boundary condition is applied to reduce computational time. Without the fully developed inlet profile, the flow needs some time to adapt to a fully developed profile, which demands computational power. The inlet boundary condition can be applied with help of Equation 18, called the power law velocity profile.

Power law velocity profile

$$u(y) = \begin{cases} U_{IN} \cdot \left[\frac{y}{D/2} \right]^{1/n}, & \text{if } y \leq \frac{D}{2} \\ U_{IN} \cdot \left[2 - \frac{y}{D/2} \right]^{1/n}, & \text{if } y > \frac{D}{2} \end{cases} \quad (18)$$

The equation is constructed of a lower and upper half since the geometry has its origin in the lower left corner. In the equation D is defined as the maximum height in the channel, U_{IN} is the maximum inlet velocity. The height of the profile can be altered by a change in U_{IN} . The power n is chosen to be 7, which is a value suited for a wide range of turbulent flows (Morrison, 2003). Figure 2 shows the analytical inlet, as presented in Equation 18, the inlet profile as extracted from the simulation and the profile at the exit of the geometry as extracted from the simulation.

One can clearly see the agreement of the analytical expression for the inlet profile with the numerical result at the inlet. The outlet however, shows a slight deviation from the inlet condition. This is due to the fact that the analytical expression is an approximation of the turbulent profile.

The second prescribed condition is the kinetic energy and

dissipation rate at the inlet of the geometry. The inlet values can be calculated upon use of Equation 19.

$$\kappa_{IN} = \frac{2}{3}(U_{IN}T_i)^2, \quad \epsilon_{IN} = C_\mu^0.25 \frac{\kappa_{IN}^{1/3}}{0.035D} \quad (19)$$

In these equations T_i is the turbulent intensity, set to a value of 4%. The value for T_i for the inlet boundary is in general taken between 1% and 6% (Versteeg and Malalasekera, 2007).

Since the focus of this problem is about the mixing quality of a turbulent flow, an important initial condition is the fractions inside the geometry. Initially the entire bottom half of the domain has a fraction $f = 1$ and the top half $f = 0$. If the fluid were to be perfectly mixed at the exit, the exit fraction would be $f = 0.5$. Therefore, the fraction is a direct measure for the mixing quality.

At both top and bottom walls of the geometry the axial velocity is set to $u = 0[m \cdot s^{-1}]$. Since the flow is turbulent not only the value at the boundary itself should be restricted, but also the so called near wall region. These regions need wall functions to describe the flow near the walls. Closest to the walls there is a viscous sub-layer. Within this layer the eddies decrease in size and dissipate their energy due to viscous forces dominating in this area. When one looks more towards the centre of the geometry a log-law layer appears. In order to implement such conditions one needs to introduce y^+ and u^+ , as seen in Equation 20 (Versteeg and Malalasekera, 2007).

$$y^+ = \frac{\rho u_\tau y}{\mu}, \quad u^+ = \frac{U}{u_\tau} \quad (20)$$

In this equation, u_τ represents the friction velocity and U is the average mean flow velocity. The friction velocity is calculated with Equation 21

$$u_\tau = \left(\frac{\tau_w}{\rho} \right)^{1/2} \quad (21)$$

τ_w is the shear stress in the boundary layer in $[Pa]$. In the viscous sub-layer, which is defined in the layer where $y^+ \leq 11.63$, the value of u^+ is equal to the value of y^+ . The shear stress in this region can be evaluated by Equation 22

$$\tau_w = \mu \frac{\partial u}{\partial y} \quad (22)$$

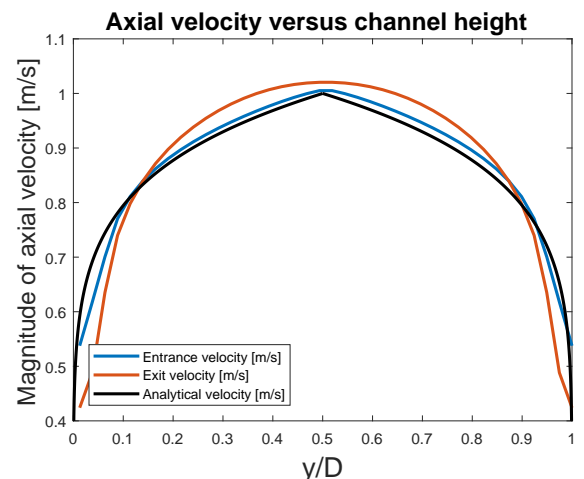


Figure 2: Schematic diagram of geometry.

If the value of the dimensionless height y^+ grows beyond 11.63 one enters the log-law regime. Within this layer u^+ is calculated with Equation 23, where the values for κ and E are 0.4187 and 9.793 respectively.

$$u^+ = \frac{1}{\kappa} \ln(Ey^+) \quad (23)$$

The shear stress in the log-law area, used to calculate y^+ , is determined upon us of Equation 24

$$\tau_w = \frac{\rho C_\mu^{0.25} \kappa^{1/2} \partial u}{u^+} \quad (24)$$

At the exit of the geometry the gradient of velocity and temperature in both u and y directions set to zero. This is done in order to comply with the mass balance equation since otherwise mass may disappear through the exit.

The velocity boundary conditions at the walls of the bluff body are treated in the same manner as explained in the previous section. Additional to that, the velocities inside the bluff body are set to zero values by prescribing $S_p = -10^{30}$. Additionally, at each of the faces of the bluff body, the a coefficient is set to zero.

RESULTS

The results of using the L^AT_EX template is a great looking paper. In Figures 1 and 1 it can be seen how figures are easily included. In Table 2 it is seen how we can include a table. The table is constructed in the file table.tex, where also the table caption and label are defined.

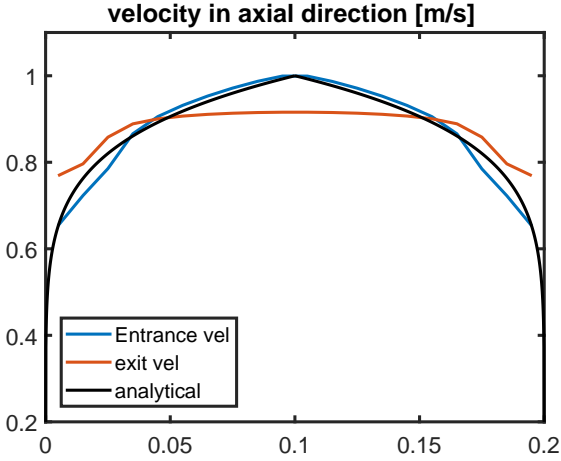


Figure 3: Turbulent inlet profile

CONCLUSION

The conclusions are:

1. Trondheim is a nice city.
2. CFD is great fun, and useful too.

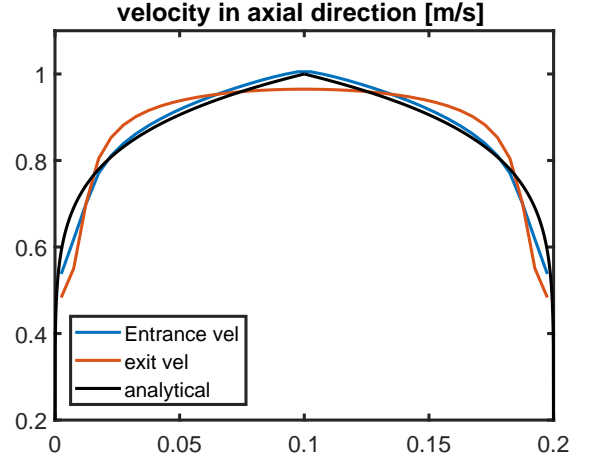


Figure 4: Turbulent inlet profile

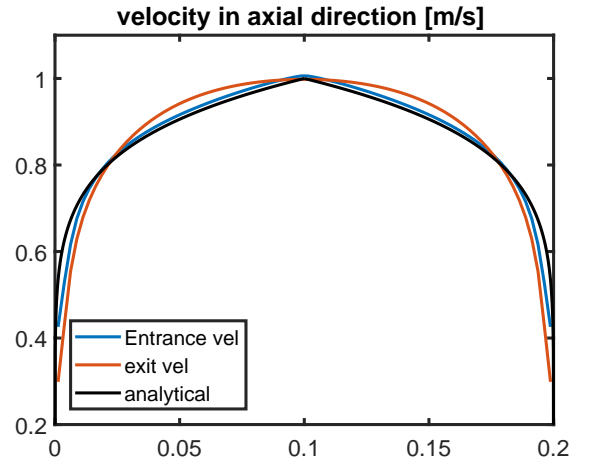


Figure 5: Turbulent inlet profile

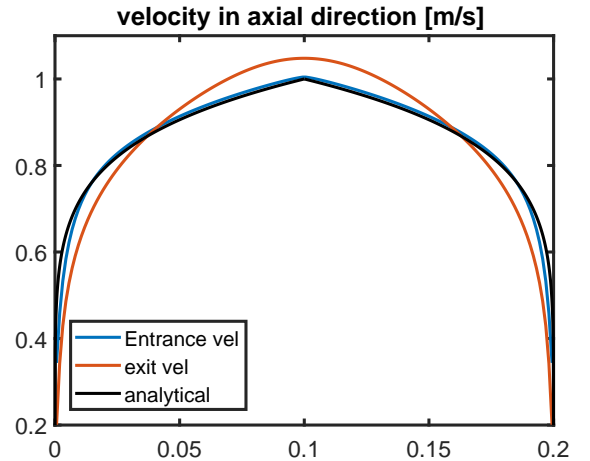


Figure 6: Turbulent inlet profile

Table 2: Modelling conditions.

| CFD Run | ω | N_D | χ_a/χ_b | $\frac{a}{b_i}$ | Γ_a | Γ_b |
|---------|----------|-------|-----------------|-----------------|------------|------------|
| First a | | | | | | |
| AA01 | 0.0391 | 0.82 | 0.9469 | 0.041 | 203 | 0.123 |
| AA02 | 0.8741 | 0.553 | 0.9528 | 0.399 | 7215 | 0.283 |
| AA03 | 0.3654 | 0.958 | 0.5304 | 0.807 | 3049 | 0.35 |
| AA04 | 0.8548 | 0.203 | 0.817 | 0.332 | 561 | 0.556 |
| AA05 | 0.8676 | 0.215 | 0.7895 | 0.509 | 9207 | 0.123 |
| AA06 | 0.1763 | 0.409 | 0.0698 | 0.995 | 7991 | 0.123 |
| First b | | | | | | |
| BA11 | 0.9654 | 0.443 | 0.5503 | 0.927 | 9257 | 0.284 |
| BA12 | 0.6548 | 0.191 | 0.5146 | 0.337 | 3357 | 0.042 |
| BA13 | 0.9476 | 0.535 | 0.2801 | 0.939 | 9389 | 0.108 |
| BA14 | 0.3063 | 0.071 | 0.364 | 0.454 | 4534 | 0.896 |
| BA15 | 0.3982 | 0.091 | 0.9544 | 0.521 | 7331 | 0.911 |
| BA16 | 0.9734 | 0.161 | 0.0897 | 0.388 | 1144 | 0.144 |
| BA17 | 0.8912 | 0.123 | 0.4564 | 0.198 | 7744 | 0.912 |
| BA18 | 0.2312 | 0.723 | 0.0218 | 0.12 | 6612 | 0.893 |
| BA19 | 0.1243 | 0.107 | 0.849 | 1.289 | 2859 | 0.698 |

APPENDIX A

Give any additional information here.

REFERENCES

- DEEN, N. (2017). “Introduction to computational fluid dynamics”.
- LI, L. and CHAN, P.W. (2012). “Numerical simulation study of the effect of buildings and complex terrain on the low-level winds at an airport in typhoon situation”.
- MORRISON, A. (2003). 32 Avenue of the Americas, New York, NY 10013-2473, USA.
- VERSTEEG, H. and MALALASEKERA, W. (2007). Edinburgh Gate, Harlow, England.

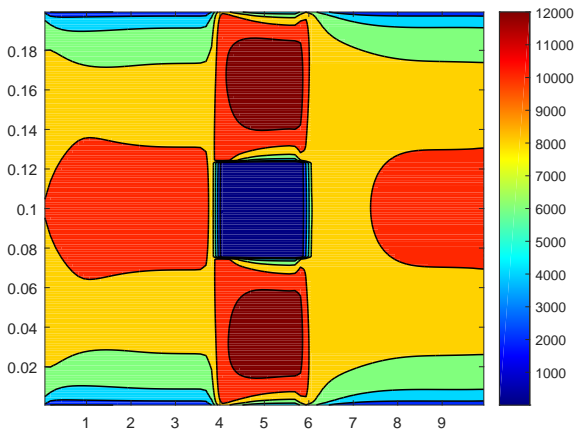


Figure 7: Reynolds number